Nuclear Engineering and Design 253 (2012) 406–412

Contents lists available at SciVerse ScienceDirect

Nuclear Engineering and Design

journal homepage: www.elsevier.com/locate/nucengdes

Interaction of a light gas stratified layer with an air jet coming from below: Large scale experiments and scaling issues

E. Studer[a,*], J. Brinster[b], I. Tkatschenko[b], G. Mignot[c], D. Paladino[c], M. Andreani[c]

[a] CEA/DEN/DANS/DM2S/SFME/LTMF 91191 Gif-sur-Yvette, France
[b] CEA/DEN/DANS/DM2S/SFME/LEEF 91191 Gif-sur-Yvette, France
[c] Thermal-hydraulics Laboratory Paul Scherrer Institute CH-5232 Villigen, Switzerland

ARTICLE INFO

Article history:
Received 7 April 2011
Received in revised form 10 October 2011
Accepted 12 October 2012

ABSTRACT

In the frame of the OECD/SETH-2 project, an experimental programme is being conducted in parallel in the PANDA facility at Paul Scherrer Institute and in the MISTRA facility at the Commissariat à l'Energie Atomique. Part of the programme focuses on gas stratification break-up induced by mass sources and similar tests have been performed in both facilities. Indeed, the scaling effect of the phenomena involved in the erosion of a gas stratified layer can be addressed. Depending on the interaction Froude number, different regimes have been identified including pure diffusive mixing, global dilution or slow erosion processes. These phenomena are driven by different time scales. Small value of the non-dimensional number leads to mixing process driven by molecular diffusion. When the interaction Froude number is increased to large values, the dilution process can be described by a global time scale based on volumetric mixing provided that the air entrainment by the jet is taken into account. The intermediate case with two layers is more complicated and a single time scale cannot be derived. These test results with high-quality measurements can be regarded as a good basis for CFD models verification.

1. Introduction and motivations

The presence of a stable light gas stratified layer in a PWR containment during the course of a severe accident is an important phenomenon for nuclear safety-related hydrogen hazard. The concentration inside this gas cloud can reach the flammability limits and the probability of occurrence of a hydrogen explosion can significantly increase. Consequently, the integrity of the containment would be threatened due to the generated overpressure and radioactive materials would be released into the environment. The conditions to obtain a stable stratified layer from a bottom-centred gaseous discharge in a closed vessel have already been addressed in the literature. The gas injection can be described by three non-dimensional numbers: the Reynolds number Re_0, the Richardson number Ri_0 and the Schmidt number Sc_0. In the following we assume that the injection Reynolds number is large enough to have a turbulent flow.

From the pioneer work of Morton et al. (1956) about jet entrainment, Baines and Turner (1969) described the different behaviour of the containment in case of plume release ($Ri_0 \gg 1$). Qualitatively, the vertical density profile outside the rising flow pattern can be divided into two or three zones. If the inertia of the rising plume is small when the flow hits the top of the vessel, a linear density gradient is obtained from the top to the bottom. Otherwise, overturning can occur and a well-mixed region is created at the top with a linear density gradient below. If the Richardson number is further reduced, overturning can involve the whole enclosure and a homogeneous atmosphere is obtained. Cleaver et al. (1994) studied this phenomenon for a methane release in an enclosure and demonstrated that stable stratification did not occur if:

$$Ri_0 < c^2 \frac{R_0^3}{H^2 V^{1/3}} \quad (1)$$

Peterson (1994) developed a similar criterion with a slightly different constant c because of partially confined conditions. Finally, in the nuclear containment thermal-hydraulics issues, Andreani et al. (2008) illustrated the set-up of a stratified atmosphere with a horizontal steam jet.

Now, we consider that the stratified layer is already set-up inside the containment and a vertical air jet is coming from below. Baines (1975) studied the jet impingement on a density interface and showed that under certain conditions this interaction results in a termination of the forward motion of the turbulent fluid. The entrainment depends only on the characteristics of the jet as it impinges and on the density difference across the interface. Three parameters are necessary to quantify this phenomenon: the velocity U and the diameter L of the jet in the impingement region and N

* Corresponding author.
E-mail address: etienne.studer@cea.fr (E. Studer).

0029-5493/$ – see front matter © 2012 Elsevier B.V. All rights reserved.
http://dx.doi.org/10.1016/j.nucengdes.2012.10.009

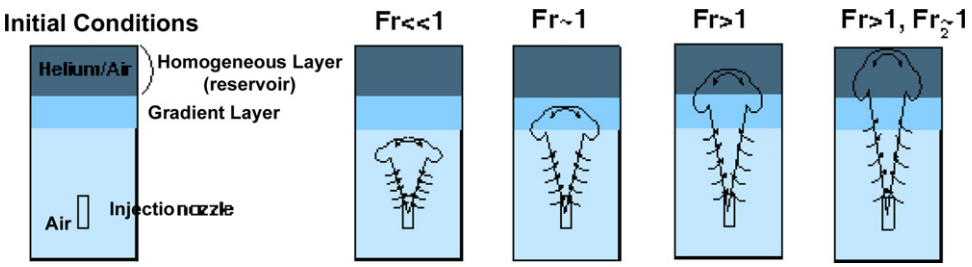

Fig. 1. Investigated flow patterns.

the characteristic pulsation of the stratification usually defined as (Jirka, 2004):

$$N = \sqrt{2g\frac{(\rho_{air} - \rho_s)}{(\rho_{air} + \rho_s)H_s}} \quad (2)$$

These parameters can be combined into one non-dimensional number called the interaction Froude number:

$$\mathrm{Fr} = \frac{U}{NL} \quad (3)$$

If this Froude number is lower than 1, buoyancy of the stratified layer dominates, and the air flow erodes the stratification without penetration (Fig. 1). For large Froude number, the momentum dominates, and the air flow penetrates inside the stratification and when the whole stratified layer is involved in this process, the phenomenon is usually called dilution. The impact velocity of the air jet at the stratified layer can be obtained by the use of well-defined correlation of velocity decay along the centreline for free jets (Rodi, 1982):

$$U = 6.2U_{inj}\frac{d_{inj}}{(z - H_{inj})} \quad (4)$$

The same reference provides the evolution of the jet diameter along the jet trajectory:

$$\frac{L}{2} = 0.086(z - H_{inj}) \quad (5)$$

From the author's knowledge, the different regimes identified during this interaction were not deeply addressed experimentally and numerically in confined geometry. Difficulties of CFD containment thermal-hydraulics codes to predict the behaviour of a stratified layer in case of an injection from below was already demonstrated during the ISP 47 exercise (Allelein et al., 2007).

The present paper is devoted to the analysis of the common tests performed in PANDA and MISTRA facilities within the OECD/SETH-2 project to address the issue presented above. Simplified tests conditions were selected for this comparison. The tests involved only air and helium mixture: a stratified layer of air/helium mixture was created at the top of both facilities. Then, air was injected vertically upward from below in order to erode the stratified layer and the transient of the mixing process was recorded with high spatial and temporal resolutions. The operating conditions were almost isothermal and at constant pressure. For comparison purpose, two tests, one at high interaction Froude number and a diffusion test have been selected at the PANDA scale whereas four tests (diffusion, low, moderate and high interaction Froude number) are considered at the MISTRA scale.

The main motivation of this work was also to compare both facilities for similar tests conditions in order to assess the scaling effect and exhibit scaling parameters as erosion in these conditions is governed by non-dimensional numbers.

After this introduction, the first section describes the facilities and the test conditions. Then, the results obtained are presented in the second section. Comparison and discussions are addressed in the last section where non-dimensional analysis and scaling parameters are exhibited. Conclusions follow.

2. Facilities and tests conditions

PANDA and MISTRA are large-scale thermal-hydraulics test facilities designed and used for investigating containment related phenomena for different Light Water Reactors designs (Auban et al., 2007; Studer et al., 2007). Two main PANDA vessels (named Vessel 1 and 2) are used in the SETH-2 project to represent nuclear reactor containment. These two vessels having each a diameter of about 4 m and a height of 8 m are interconnected by a pipe of about 1 metre diameter. The vessel 1 (Fig. 2, right) is mainly used in the present experiments. MISTRA facility is a single vessel (Fig. 2, left) with almost the same length scales (4.25 m inner diameter and a height of 7.4 m). A compartment consisting of an inner cylinder with an annular floor located approximately at mid elevation was installed inside the main vessel.

Location of gas concentration sensors (sampling tubes for PANDA, sampling tubes and mini-katarometers for MISTRA) is reported on Fig. 2. They were distributed along the stratified layer in both facilities. In the PANDA tests, measurements were conducted in the alignment of the air injection near the wall as well as in the central axis. In the MISTRA facility, the mini-katarometers and the injection were located in the annular ring not along the centreline of the facility.

The main test conditions are reported in Table 1 for both facilities. The boundary and initial conditions are almost the same except the distance between the injection location and the bottom of the stratified layer (2200 mm in the MISTRA test conditions and 875 mm in the PANDA test conditions). Slightly heated air was also injected in the PANDA experiments compared to the MISTRA ones.

The stratified layer of light gas in the top of both facilities is plotted in Fig. 3. The shape is equivalent but the location is slightly different. Especially, the helium reservoir in the top of the facility is more important in the PANDA test.

Non-dimensional Froude number can be calculated based on the initial and boundary conditions of the tests (Table 2). According to the hypothesis of the calculations, the interaction Froude number

Table 1
Initial and boundary conditions for PANDA and MISTRA tests.

Data	PANDA	MISTRA	Unit
Injection diameter (d_{inj})	75	72	mm
Injection height (H_{inj})	4013	3660	mm
Elevation of the top of the facility (H_F)	7984	7379	mm
Elevation of the bottom of the stratified layer (Z_{min})	4875	5800	mm
Height of the stratified zone (H_s)	1250	1300	mm
Total pressure	0.974	1.005	bar
Temperature	288	292	K
Injected air flow (Q_{air})	15	4.5–50.6	g/s
Injected air temperature (T_{air})	303	292	K

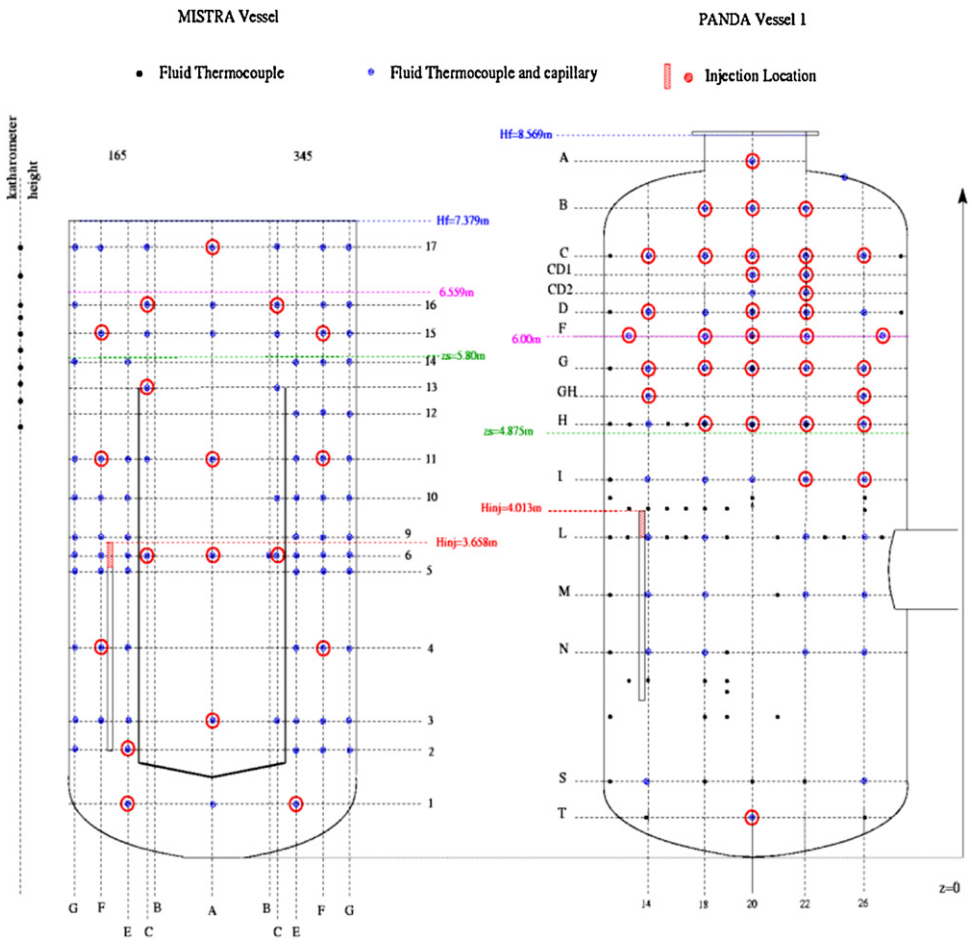

Fig. 2. View of MISTRA and PANDA facilities with sensors locations.

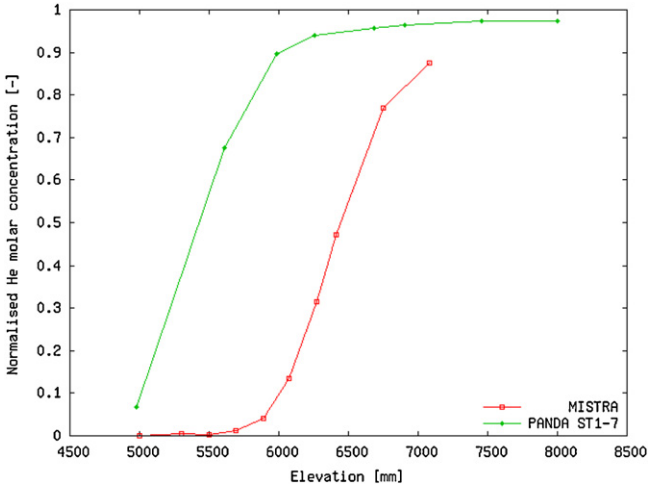

Fig. 3. Stratified layer at $t = 0$ in both facilities PANDA and MISTRA.

Table 2
Non-dimensional analysis for PANDA (ST1_7) and MISTRA (LOWMA series).

Test	Q_{air} (g/s)	U_{inj} (m/s)	U (m/s)	z (m)	N (/s)	L (m)	Fr	Fr_2
ST1_7	15.02	3.03	1.64	0.86	1.83	0.15	6.04	0.49
LOWMA2	4.53	0.93	0.19	2.14	1.75	0.37	0.30	0.08
LOWMA3	15.17	3.11	0.65	2.14	1.75	0.37	1.00	0.29
LOWMA4	50.58	10.36	2.16	2.14	1.75	0.37	3.35	0.96

covers a large range between 0.3 and 6. The PANDA test ST1-7 is more momentum dominated than the corresponding MISTRA test (LOWMA3). Nevertheless, due to the large helium reservoir at the top of PANDA facility, the penetration of the air jet can be limited to a certain extend and the global dilution of the stratified layer cannot be achieved very quickly (Fig. 1). A second Froude number (Fr_2) based on the interface gradient has been defined in order to take into account this reservoir effect:

$$Fr_2 = \frac{U}{\sqrt{g((\rho_s - \rho_{air})/\rho_{air})(H_F - Z_{min})}} \quad (6)$$

According to this new non-dimensional number, the PANDA ST1-7 test is between the MISTRA LOWMA3 and LOWMA4 tests and the latter corresponds to a Froude number close to unity recalling that inertia of the impinging jet is equivalent to the buoyancy of the stratified layer. It should be pointed out that this calculated Froude numbers are based on ideal initial conditions and that, for the duration of the test, it changes. For example, if an erosion process is assumed, the actual layer will move upward and a decrease in the Froude number at the interface would be observed.

3. Panda and mistra results

Two tests were run in the PANDA facility named ST1-7 and ST1-7-2. An additional reference diffusion test has also been conducted for comparison with the initially conducted tests ST1-7 and ST1-7-2. Even though the initial concentrations were slightly different, the two tests gave comparable results and only ST1-7 will be here compared to the corresponding diffusion test and the MISTRA results.

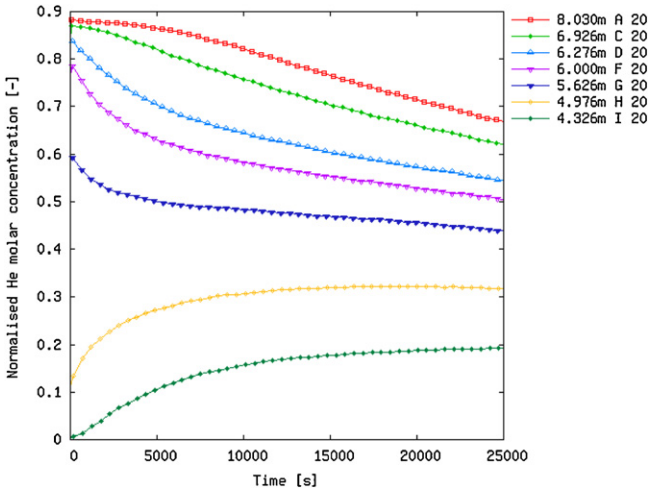

Fig. 4. Results of PANDA diffusion test – Helium concentration along the centreline versus time.

The diffusion test was conducted with both vessels isolated from environment for a period of three days. The time evolution of the helium molar fraction along the central axis is plotted in Fig. 4. Only the first 25,000 s are shown here. During the first 5000 s very little helium is diffused from the upper part of vessel 1 (Level A). This test should be compared with ST1-7 presented in Fig. 5. During the process of mixing, well-mixed conditions are achieved up to a certain elevation that grows with time, from 5.6 m at 1000 s to 6.93 m at 12,000 s. The helium content in this well-mixed layer decreases with time due to the continuous dilution induced by the injected air. Two sensors located at the top of the facility (A and B) cannot reach these well-mixed conditions during the process of air injection. When the air injection is stopped (12,500 s), a splitting of the gas concentration measurements in the layers below 6.93 m is observed. After the damping of the convection effect in the vessel, this would correspond once again to a pure diffusive process due to helium coming from above.

Both tests can be compared by normalising the helium molar fraction with the corresponding maximum value. Fig. 6 clearly shows that the upper layers are initially governed by pure diffusive process. More than 5000 s of air injection are needed before that the helium concentration evolution deviates from the pure diffusion evolution. It is in the range of 2000 s for C level and around 300 s for the level F. This means that the upper layer does not see

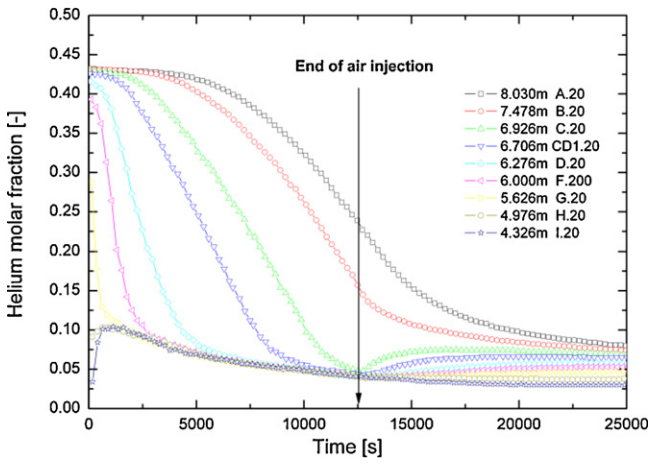

Fig. 5. Results of PANDA ST1-7 test – Helium concentration along the centreline versus time.

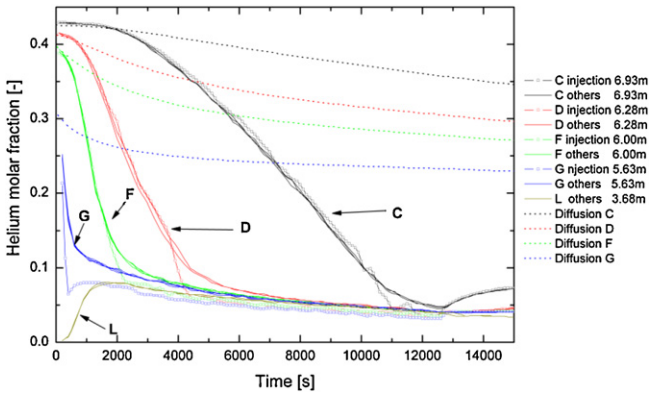

Fig. 6. Impact of air jet on the helium layer (PANDA ST1-7).

the impact of the air jet until late in the experiment and that also, despite an initial Froude number larger than one, the air jet does not penetrate deeply in the layer initially. The effect of the impact of the jet on the layer can also be observed by comparing the helium concentration measurements along the air injection axis (denoted as 14 in PANDA nomenclature) and off axis (denoted 18, 20, 22 or 26 in PANDA nomenclature). For a given elevation, an earlier drop of the concentration along the injection axis is observed compared to the rest of the layer off injection axis. Also, the time at which the concentration along the injection axis departs from the others locations give information on the penetration depth of the air jet. For C level ~10,000 s, for D level ~3700 s and for F level ~1500 s. One final remark concerns the fact that the dilution process slows down for each level as soon as the jet as reach the corresponding level height, in other words, right after the departure time given previously.

Different tests including reproducibility were performed in the MISTRA facility in order to follow the behaviour of the stratified layer created initially (Brinster et al., 2009). In the first experiment (diffusion test), no air injection was imposed and the erosion of the helium layer by diffusive process was recorded (Fig. 7). The profiles are similar to those observed in the PANDA diffusion test and a good agreement is obtained with a 2D solution of pure molecular diffusion process performed with the CAST3M CFD computer code. In the simulation, the diffusion coefficient of helium in air is set to $6.98.10^{-5}$ m^2/s according to Marrero and Mason (1972).

When air is injected below the stratified layer, modification of the transient behaviour is expected. Nevertheless, if the air flow

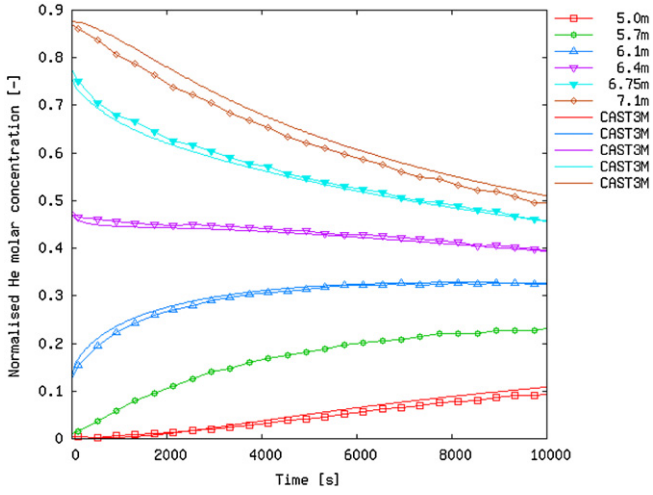

Fig. 7. Results of MISTRA diffusion test – Helium concentration along the centreline.

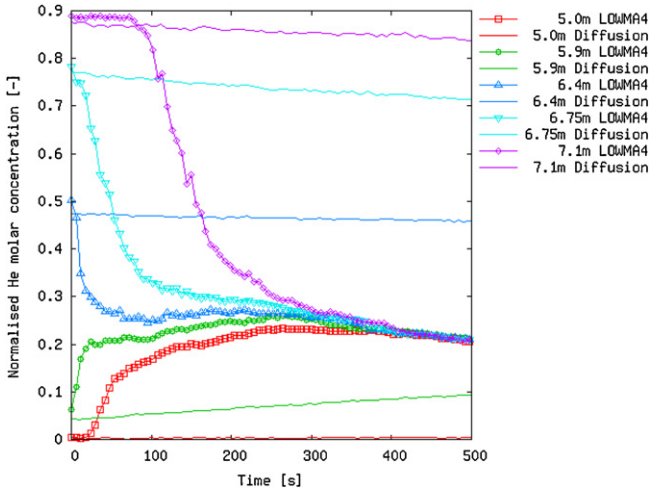

Fig. 8. Results of MISTRA test with high interaction Froude number – Helium concentration along the centreline.

rate is small (LOWMA2 test) namely the interaction Froude number is small (0.3 in this case), the erosion of the stratified layer is still governed by the diffusion phenomena. There was no noticeable difference between LOWMA2 results and the diffusion results. In each LOWMA test, the air injection was stopped after 6000 s.

Large interaction Froude number leads to a rapid break-up of the stratified layer (Fig. 8). Just after the beginning of air injection, the layers up to 6.75 m are impacted by the dilution process. The erosion of the upper layer (7.1 m) is first driven by the diffusion process during about 300 s and then dilution process involves the whole layer. Such delay has also been observed in the PANDA results (F level).

In the critical range Fr ~ 1, the injected air starts to dilute the lower layers of the air/helium cloud and then, the diffusion process is enhanced by this convective contribution. This clearly appears on Fig. 9. It is also interesting to notice that due to the small depth of the air/helium cloud in the MISTRA facility, shorter delays in the behaviour of the upper layers are observed compared to the PANDA results. The sensors located around 6 m show first the effect of the injection and this is probably due to the off-centred injection and the off-centred location of the measurement devices. Then, sensors located below 6 m need some delay to reach almost well-mixed conditions. Above 6 m, all the sensors especially at 6.1 and 6.25 m

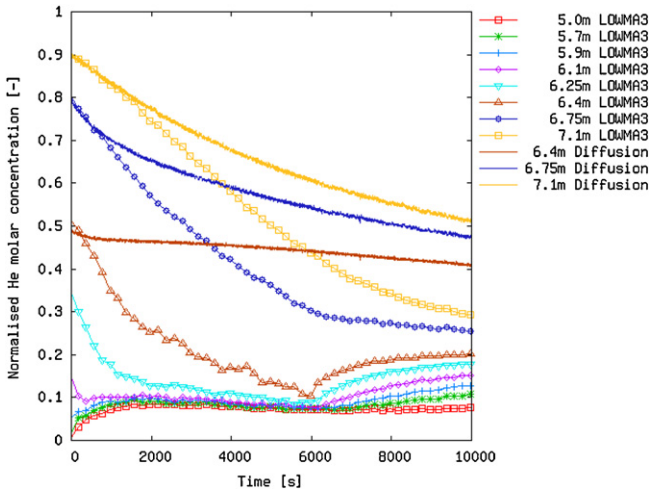

Fig. 9. Results of MISTRA LOWMA3 test with intermediate interaction Froude number.

elevations record decreasing helium concentration due the dilution effect of the lower layers. At the end of the air injection (6000 s), the well-mixed conditions extend to 6.25 m and the upper part of the facility remains stratified.

4. Comparison and discussions

4.1. Local analysis

Direct comparison of the measurements is difficult due to some differences listed previously (height of the injection line compared to the bottom of the stratified layer, slightly heated air jet, different depth of the stratified layer). Comparison between tests performed in both facilities requires non-dimensional quantities. Gas concentrations fulfil this requirement and characteristic time scales have to be defined.

Different time scales can be defined according to the experimental results and the expected physical phenomena:

- t_{dif} corresponds to homogenisation by molecular diffusion of the gaseous volume inside the facility. It is relevant for zones where molecular diffusion is dominant.
- A second time scale can be derived from the initial and boundary conditions $t_{air} = V_{cloud}/Q_{(v,air)}$ where V_{cloud} is the equivalent volume of injected helium and $Q_{(v,air)}$ is the volumetric flow of injected air. This time scale is related to dilution effect in zones where convection is dominant.
- The third time scale t_{dep} is derived from the experimental results for zones between convection and diffusion dominant regions. The experimental results have shown that some sensors located in these intermediate zones follow a diffusion profile for a certain duration called t_{dep}.

The 2D CFD computations with CAST3M code have demonstrated that the time scale t_{dif} assuming that 90% of the well-mixed conditions are achieved is almost the same in both facilities (about 200,000 s). So, long term comparison can be directly performed and two sensors located in the diffusive region during LOWMA3 (6.4 and 7.1 m elevation) and ST1-7 tests (6.71 and 7.48 m elevation) show approximately the same transient behaviour provided that a time synchronisation is made based on a common initial gas concentration value.

For the LOMWA3 and ST1-7 tests, the values of t_{air} are 451 and 933 s, respectively. The factor of 2 corresponds to the difference in the volume of helium stored at the top of the facility. For this short term analysis, the test LOWMA4 has been selected and the comparison is performed with the PANDA ST1-7 results. In these two tests, the interaction Froude number is high enough to break-up the stratified layer. Two sensors with approximately the same initial helium content have been chosen for comparison (Fig. 10). The results seem to indicate that the selected time scale is the adequate reference time scale for short term behaviour (dilution dominated mixing process).

Finally, the third time scale t_{dep} is obtained for the upper layers in the different tests (Figs. 6, 8 and 9). Fig. 11 summarises the results. When Fr_2 increases, the slope also increases indicating faster phenomenon and the PANDA result lies in between the two MISTRA results.

4.2. Global analysis

Let us define Z_{min} the elevation located at the bottom of the stratified layer. Above this elevation a certain amount of helium is initially stored. This light gas mixed with air aimed at representing a flammable cloud that may be created during the course of a severe

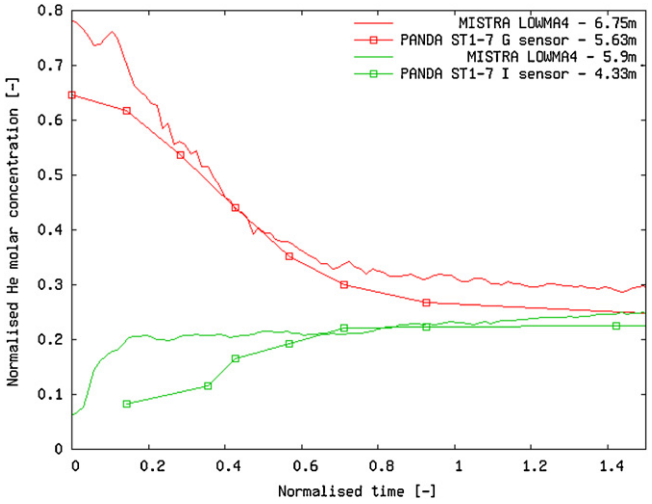

Fig. 10. Comparison for local Helium concentration and short time scale (t_{air}).

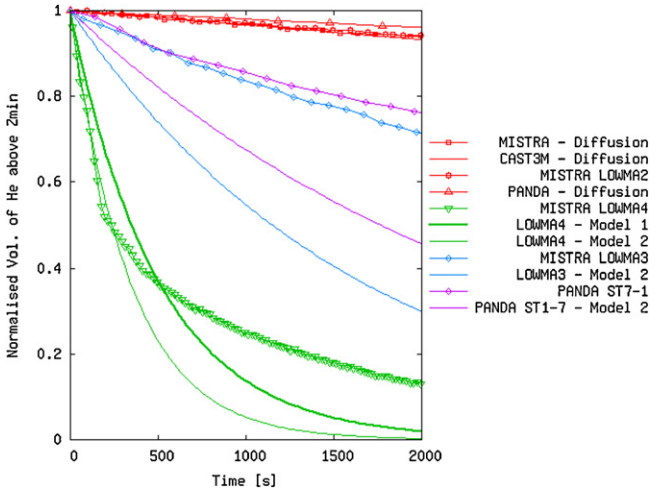

Fig. 12. Global analysis – evolution of the helium volume above Z_{min} versus time.

accident in the containment of a nuclear reactor. The flammable cloud size can be represented by the global variable V_{cloud} which accounts for the volume of flammable gas above Z_{min}. In our case V_{cloud} represents the volume of helium in the layer and corresponds initially to the volumetric equivalent of the injected mass of helium. The erosion effect of any phenomenon can be represented by the time evolution of V_{cloud}. The objective is to decrease the volume beyond the flammability limits. This is a global criterion and then, the local flammable gas concentration has also to be decreased below the lower flammability limit.

The weakest phenomenon to drive the erosion process is the molecular diffusion. Helium is swept out of the stratified layer and air slowly diffuses inside. Assuming axial symmetry, the time evolution of V_{cloud} caused by molecular diffusion can be solved analytically. In the present document, we use the CAST3M simulations previously mentioned to compute the time evolution of this volume. A relative good agreement is obtained between the experimental results and the molecular diffusion computation (Fig. 12) for the LOWMA2 and diffusion tests.

When air is injected from below, convection starts to play a significant role to the dilution or erosion process. The simplest way to model the air injection is to suppose that the whole layer is diluted by the entire air flow. This leads to well-mixed conditions and the volumetric balance of helium can simply be written as:

$$\frac{dV_{cloud}}{dt} = -\frac{Q_{(v,air)}}{V} V_{cloud} \tag{7}$$

with the solution of:

$$V_{cloud}(t) = V_{cloud}(0) \exp\left(-\frac{Q_{(v,air)}}{V} t\right) \tag{8}$$

This first approach (called Model 1) is too simple because in the free jet theory, the volumetric flow is not conserved along the trajectory of the jet. Outside air/helium is entrained into the rising jet. The balance equation can be expressed as:

$$\frac{dQ}{ds} = \alpha_1 U \pi L \tag{9}$$

with L the jet diameter, U the jet centreline velocity, s the coordinate along the trajectory and α_1 the entrainment coefficient (0.055 for a pure jet). By the use of classical correlations for the jet centreline velocity decay and the half-width growth, the air flow injected in the stratified layer can be estimated properly.

$$\frac{dQ}{ds} = \alpha_1 \left(6.2 U_{inj} \frac{d_{inj}}{s}\right) \pi 0.164\,s = 4,07 \alpha_1 \frac{Q_{(v,air)}}{d_{inj}} \tag{10}$$

So, the volumetric flow of air increases linearly with s and depends only on the injection conditions. This last model (Model 2) is very close to the LOWMA4 experimental results at the beginning of the transient (Fig. 12) where the slope is accurately captured. For the rest of the transient, since confined or semi-confined conditions are involved, helium is certainly entrained by the air jet and our simplified hypotheses are no longer valid. As a consequence, the time scale is longer in the experiments compared to the simplified models.

Between the two limiting cases, phenomena are more complex because the interaction of the rising jet and the stratified layer occurs at a certain level above Z_{min} and probably changes in time due to the erosion process. This is the case in the PANDA ST1-7 and MISTRA LOWMA3 tests where the behaviour of the erosion process is between pure diffusion and global dilution (Fig. 11). The characteristic time scales defined before are not accurate to compare the two facilities. The two experimental curves are identical up to 500 s and then a slight deviation can be observed: the ratio between the characteristic time scale of PANDA and MISTRA is about 1 for short time and 1.5 for long term. So, a single time scale cannot be obtained for this global parameter.

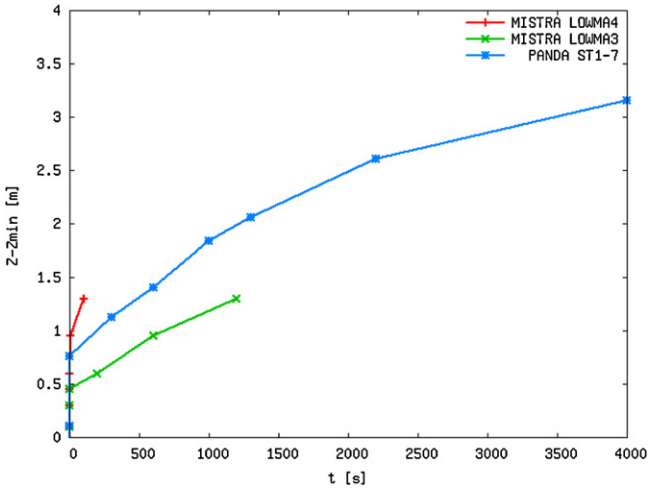

Fig. 11. Local analysis – departure time (t_{dep}) from a pure molecular diffusive process at a given elevation.

5. Conclusions and perspectives

Interesting phenomena have been experienced in both PANDA and MISTRA facilities. Interaction of a fountain like flow with a stratified layer is a complex phenomenon. The different regimes including pure molecular diffusion mixing, global dilution and slow erosion process have been observed and analysed based on local and global behaviour. Dimensionless quantities have been proposed. The interaction Froude number can be used to identify the ability of the air jet to erode or to dilute the stratified layer. A second Froude number has been proposed to analyse the effect of the layer width. The Froude number has to be considered with care as it is calculated for initial condition only. It evolves with time leading to change in erosion process along the test and this is truer for PANDA due to the important helium reservoir on top of the facility. Regarding the time scale, small interaction Froude number leads to mixing process driven by molecular diffusion. When the interaction Froude number is increased to large values, the dilution process can be described by a global time scale based on volumetric mixing (t_{air}) provided that the air entrainment by the jet is taken into account. The intermediate case with two layers is more complicated and a single time scale cannot be derived. These tests results can be regarded as a good basis for CFD models verification.

Acknowledgments

The authors gratefully acknowledge the support of all the countries and the international organisations participating in the OECD/SETH-2 project.

References

H.J. Allelein, K., Fischer, J., Vendel, J., Malet, E., Studer, S., Schwarz, M., Houkema, H. Paillère, A. Bentaib, 2007. International Standard Problem ISP-47 on Containment Thermal-hydraulics, NEA News. 25 (2).

Auban, O., Zboray, R., Paladino, D., 2007. Investigation of large-scale gas mixing and stratification phenomena related to LWR containment studies in the PANDA facility. Nucl. Eng. Des. 237, 409–419.

Andreani, M., Haller, K., Heitsch, M., Hemström, B., Karppinen, I., Macek, J., Schmid, J., Paillère, H., Toth, I., 2008. A benchmark exercise on the use of CFD codes for containment issues using best practice guidelines: a computational challenge. Nucl. Eng. Des. 238, 502–513.

Baines, W.D., Turner, J.S., 1969. Turbulent buoyant convection from a source in a confined region. J. Fluid Mech. 37, 51–80 (part 1).

Baines, W.D., 1975. Entrainment by a plume or jet at a density interface. J. Fluid Mech. 68, 309–320 (part 2).

J. Brinster, D., Abdo, E., Studer, I., Tkatschenko, J.L. Widloecher, 2009. OECD/SETH-2 project: synthesis report for MISTRA INITIALA/LOWMA test. CEA Technical Report.

Cleaver, R.P., Marshall, M.R., Linden, P.F., 1994. The build-up of concentration within a single enclosed volume following a release of natural gas. J. Hazard. Mater. 36, 209–226.

Jirka, G.H., 2004. Integral model for turbulent buoyant jets in unbounded stratified flows. Part I: single round jet. Environ. Fluid Mech. 4, 1–56.

Marrero, T.R., Mason, E.A., 1972. Gaseous diffusion coefficients. J. Phys. Chem. Ref. Data 1, 3–83.

B.R. Morton, S.G., Taylor, J.S. Turner, 1956. Turbulent gravitational convection from maintained and instantaneous sources. Proc. R. Soc. Lond. Ser. A: Math. Phys. Sci. 234 (1196) 1–23.

Peterson, P.F., 1994. Scaling and analysis of mixing in large stratified volumes. Int. J. Heat Mass Transfer 37 (suppl 1), 97–106.

Rodi, W. (Ed.), 1982. HMT the science & applications of heat and mass transfer. in: Turbulent Buoyant Jets and Plumes, vol. 6., 1st edition Pergamon Press.

Studer, E., Magnaud, J.P., Dabbene, F., Tkatschenko, I., 2007. International standard problem on containment thermal-hydraulics ISP47: Step 1 – results of the MISTRA exercise. Nucl. Eng. Des. 237, 536–551.